# Analysis of the Side-lobes of FBG Reflection Spectra From Matrix Cracks in Composites

**Aydin Rajabzadeh[a,b], Richard Heusdens[a], Richard C. Hendriks[a], and Roger M. Groves[b]**

[a] *Circuits and Systems group of Electrical Engineering Department of Delft University of Technology, Delft, 2628 CD, The Netherlands* [b] *Structural Integrity and Composites group of Faculty of Aerospace Engineering Department of Delft University of Technology, Delft, 2629 HS, The Netherlands*

*{A.Rajabzadehdizaji, R.Heusdens, R.C.Hendriks, R.M.Groves}@tudelft.nl*

**Abstract:** The previously described approximated transfer matrix model (ATMM) provides insight into the strain distribution along on fibre Bragg grating (FBG) sensor. In this paper we study the influence of matrix cracks in composites on the angular frequency of the side-lobes of the FBG reflection spectra in frequency space. 

**OCIS codes:** 060.3735, 070.2025, 050.1755, 130.6010, 280.4788.

## 1. Introduction

Fibre Bragg grating (FBG) sensors are traditionally used for point strain and temperature, vibration and pressure measurement [1]. In addition, there has recently been an increased interest in using FBG sensors for the detection of impact damages. This can be accomplished via dynamic measurements of the Bragg wavelength shifts of the FBG at the time of the impact [2], or by analysing the static response of the FBG after the event [3]. This current study belongs to the latter group. We present an analytical model for the reflection spectra from an FBG sensor embedded in a composite structure which is mechanically loaded to induce matrix cracking. While previous studies have been based on the extraction of statistical features [2, 3], in this paper we follow an analytical approach and derive a model that can be used to detect cracks in proximity to the active length of the FBG sensor.

We consider an FBG sensor embedded between the layers of a healthy carbon fibre reinforced plastic (CFRP) composite structure. Due to the brittle nature of the matrix material, an impact can result in matrix cracking. Some of these cracks will be adjacent to the active length of the embedded FBG sensor. In such a case, the strain distribution will show sharp amplitude changes along the length of the sensor, with local maxima at the crack location [4]. In order to visualise this phenomenon, consider the schematic diagram of a virtual FBG sensor embedded between two perpendicular layers of a unidirectional carbon fibre composite structure shown in Fig. 1a. Due to the presence of the cracks and considering the mechanical properties of the composite laminates, McCartney's theory for $\sigma_z = 400$ MPa can be used to calculate the strain distribution along the length of the sensor, which is shown in Fig. 1b [4].

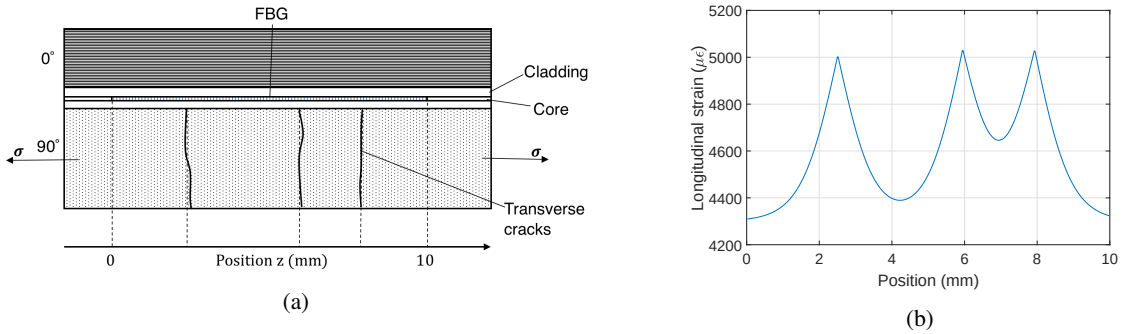


Fig. 1. (a): A schematic of the formation of cracks in the proximity of an embedded FBG between layers of a composite panel (b): The strain distribution along the length of the FBG, calculated using McCartney's theory for $\sigma_z = 400$ MPa.

In [5] we presented a model for the analysis of FBG reflection spectra under non-uniform strain fields. Based on this model, we presented a robust algorithm for calculating the mean strain of such non-uniform strain fields using a (uniform) FBG sensor. Another direct result of this model was a closed-form approximation of the side-lobes of the

FBG reflection spectra. In [5] we showed that in particular, these side-lobes carry important information about the mean strain. Based on the model proposed in [5], we will show in this paper how we can derive an analytical model for the FBG reflection spectra when the composite contains matrix cracks. Similar as the model presented in [5], characterising these microscopic cracks is based on analysing the side-lobes of the FBG reflection spectra.

## 2. Approximated Transfer Matrix Model (ATMM)

FBG sensors have the important property that the shift of the Bragg wavelength changes linearly with the amount of strain for a uniform axial strain distribution along the length of the sensor. Using coupled mode theory [6], one can derive a closed form equation that characterises the reflection spectrum of the FBG under uniform fields. However, when the strain field is non-uniform, the analytical expression for the reflection spectrum becomes much more complicated, and modelling it using the coupled mode theory becomes rather cumbersome. A common way to tackle this problem is to use the transfer matrix model, where the length of the FBG sensor is discretised into several smaller piecewise uniform segments. In 1989, Yamada and Sakuda formulated the transfer matrices, and also the relations between the forward and backward electric waves, propagating through the waveguide [7]. Based on the transfer matrix model, we proposed in [5] a new model that approximates the transfer matrices to a simpler and more compact form, capable of extracting more information about the strain field the sensor is subjected to [5]. Similar to the transfer matrix model, we assumed the length of the sensor has been divided into $M$ smaller piecewise uniform segments with length $\Delta z$. The forward propagating electric wave entering the $i$'th segment will be called $A_i$, and the backward propagating electric wave, reflected from the $i$'th segment will be called $B_i$. In [5] we showed that for small enough $\Delta z$, the relationship between the forward and backward electric waves is characterised by the following relations.

$$\begin{pmatrix} A_i \\ B_i \end{pmatrix} = F_i \begin{pmatrix} A_{i-1} \\ B_{i-1} \end{pmatrix}, \qquad \text{with} \qquad F_i = \begin{pmatrix} e^{-j(\alpha-\alpha_i)} & -j\kappa_i \Delta z \,\mathrm{sinc}(\alpha-\alpha_i) \\ j\kappa_i \Delta z \,\mathrm{sinc}(\alpha-\alpha_i) & e^{j(\alpha-\alpha_i)} \end{pmatrix}. \tag{1}$$

$F_i$ is the approximated transfer matrix of segment $i$ with elements $F_{i_{11}}$, $F_{i_{12}}$, $F_{i_{21}}$ and $F_{i_{22}}$. In these relations $\kappa_i$ is the coupling coefficient between the forward and backward waves,

$$\alpha = \frac{2\pi n_{\text{eff}} \Delta z}{\lambda} \quad \text{and} \quad \alpha_i = \frac{2\pi n_{\text{eff}} \Delta z}{\lambda_i}. \tag{2}$$

In these relations, $\lambda$ is the wavelength range under analysis, $\lambda_i$ is the Bragg wavelength of the $i$'th segment, and $n_{\text{eff}}$ is the effective refractive index of the core. It can be seen that the relation between the electric waves in the first and the last segments can be derived as

$$\begin{pmatrix} A_M \\ B_M \end{pmatrix} = F \begin{pmatrix} A_0 \\ B_0 \end{pmatrix}, \quad \text{in which} \quad F = \prod_{i=1}^{M} F_i. \tag{3}$$

With the assumption that there is full transmission of the incident light in the last segment and no reflection from further along the length of the sensor, i.e., $A_0 = 1$ and $B_0 = 0$, the reflection spectrum, say $R(\lambda)$, can be calculated as

$$R(\lambda) = \left| \frac{B_M}{A_M} \right|^2 = \left| \frac{F_{21}}{F_{11}} \right|^2. \tag{4}$$

### 2.1. *Closed Form Approximation of the Side-lobes*

Suppose an arbitrary non-uniform strain field is applied to the length of the sensor. In [5] we showed that under such conditions, the reflection spectra for wavelengths $\lambda$ that are sufficiently far away from the Bragg wavelength $\lambda_B$ can be approximated by

$$R(\lambda) \approx \left| \sum_{i=1}^{M-1} (\xi_i - \xi_{i+1}) e^{-j\left((M-2i)\alpha + \sum_{k\le i}\alpha_k - \sum_{k>i}\alpha_k\right)} + \left( \xi_M e^{jM(\alpha-\bar{\alpha})} - \xi_1 e^{-jM(\alpha-\bar{\alpha})} \right) \right|^2, \text{ for } |\lambda - \lambda_B| > \lambda_{\text{th}}, \tag{5}$$

where $\lambda_{th} > 0$ is a threshold for which Eq. (5) holds, $\bar{\alpha} = \sum_{i=1}^{M} \alpha_i / \mathrm{M}$, and $\xi_i = \frac{\kappa_i \Delta z}{2j(\alpha-\alpha_i)}$. The particular $\lambda$ range for which the approximation in Eq. (5) holds corresponds with the side-lobes of the reflection spectra. In [5] we showed that when the strain distribution is smooth (i.e., no sudden change of the strain in consecutive segments) $\xi_i - \xi_{i+1}$ is much smaller than $\xi_m$ or $\xi_1$, and that as a consequence, the summation in Eq. (5) will be negligible compared to the

other terms. For the rest of this paper, we consider the region where $\lambda - \lambda_B > \lambda_{th}$, which satisfies the condition in Eq.( 5). Under smooth (but not necessarily uniform) strain distributions we have from Eq.(5)

$$R_s(\lambda) \approx |\xi_1|^2 + |\xi_M|^2 - 2\mathrm{Re}[\xi_1 \xi_m^*]\cos(2M(\alpha - \bar{\alpha})). \tag{6}$$

When the strain distribution is not only smooth, but also uniform (i.e., $\forall i,\ \xi_i = \bar{\xi}$), the summation in Eq. (5) will be exactly zero, and the reflection spectra can be approximated as

$$R(\lambda) \approx \left| \bar{\xi} e^{jM(\alpha-\bar{\alpha})} - \bar{\xi} e^{-jM(\alpha-\bar{\alpha})} \right|^2 = (\kappa L)^2 \,\mathrm{sinc}^2\left(M(\alpha - \bar{\alpha})\right), \qquad \text{for } |\lambda - \lambda_B| > \lambda_{\mathrm{th}}, \tag{7}$$

## 3. Detection of Matrix Cracks

When the active length of the FBG sensor is in contact with matrix cracks transversal to its longitudinal axis, sudden strain changes in consecutive segments of the FBG structure will appear at the locations of the cracks. Let us for simplicity assume there is only one single transverse crack present, which is located at the $t$'th segment of the FBG structure. This means that there will be a sudden change of strain from segment $t-1$ to $t$ and also from segment $t$ to segment $t+1$, along with a smoothly varying strain distribution over the other segments of the model. Therefore, neglecting the terms in Eq. (5) where the consecutive $\xi_i$ values are rather similar, we obtain

$$R_c \approx \left| \sum_{i=t-1}^{t} (\xi_i - \xi_{i+1})\, e^{-j\left((M-2i)\alpha + \sum\limits_{k\le i}\alpha_k - \sum\limits_{k>i}\alpha_k\right)} + \left( \xi_M e^{jM(\alpha-\bar{\alpha})} - \xi_1 e^{-jM(\alpha-\bar{\alpha})} \right) \right|^2, \qquad \text{for } |\lambda - \lambda_B| > \lambda_{\mathrm{th}}, \tag{8}$$

where, compared to Eq. (7) we have a contribution of the $\xi_i$ values around the $t$th segment due to the crack in segment $t$. With this, the reflected side-lobe spectrum $R$ can be written as

$$R_c \approx R_s + \psi_0 + 2\overbrace{\mathrm{Re}[(\xi_{t-1} - \xi_t)\xi_M^*]}^{\psi_1}\cos\left((2M - 2t + 2)\alpha + \theta_1\right) - 2\overbrace{\mathrm{Re}[(\xi_{t-1} - \xi_t)\xi_1^*]}^{\psi_2}\cos\left((2t-2)\alpha + \theta_2\right) + \tag{9}$$
$$2\overbrace{\mathrm{Re}[(\xi_t - \xi_{t+1})\xi_M^*]}^{\psi_3}\cos\left((2M-2t)\alpha + \theta_3\right) - 2\overbrace{\mathrm{Re}[(\xi_t - \xi_{t+1})\xi_1^*]}^{\psi_4}\cos\left(2t\alpha + \theta_4\right) + 2\overbrace{\mathrm{Re}[(\xi_t - \xi_{t+1})(\xi_{t-1} - \xi_t)^*]}^{\psi_5}\cos\left(2\alpha + \theta_5\right),$$

where $\psi_0$ stands for the real value of a non-linear combination of the $\xi_i$ parameters with no modulation, $\theta_i$ terms are linear combinations of the $\alpha_i$ parameters, and $\mathrm{Re}[\cdot]$ stands for the real part of the complex value. In addition, because $\xi_{i-1} - \xi_i$ is typically smaller than $\xi_1$ or $\xi_M$, usually the term $\psi_5$ in Eq. (9) is relatively small compared to the other terms. Comparing $R_c$ with $R_s$ in Eq. (6), it can be seen that the presence of a single crack reflects itself as five new harmonic terms ($\psi_1$ till $\psi_5$). Note that all crack related harmonics have lower frequencies than the already existing harmonic in $R_s$ (with angular frequency $2M\alpha$). Due to the decaying nature of the side-lobes of the reflection spectrum (with an inverse square rate of decay), using a rectangular window on the side-lobes will result in broadened peaks and also spectral leakage in the Fourier domain. In order to resolve this problem, and also to avoid the ambiguity of defining a proper range for the side-lobes (defining a proper $\lambda_{th}$), we propose replacing the rectangular window with a non-linearly scaled Hann window of the form:

$$w = \frac{1}{2}\left(1 + \cos\left(\frac{2\pi(\alpha - \alpha_c)}{\alpha_{\mathrm{ub}} - \alpha_{\mathrm{lb}}}\right)\right)(\alpha - \alpha_B)^2, \qquad \text{for } \lambda_{\mathrm{lb}} < \lambda < \lambda_{\mathrm{ub}}, \tag{10}$$

where $\alpha_B$ is a scalar, corresponding to the Bragg wavelength of the stressed sensor, $\alpha_c$ corresponds to $(\lambda_{\mathrm{ub}} + \lambda_{\mathrm{lb}})/2$, $\alpha_{\mathrm{lb}}$ and $\alpha_{\mathrm{ub}}$ correspond to $\lambda_{\mathrm{lb}}$ and $\lambda_{\mathrm{ub}}$. The values of $\lambda_{\mathrm{lb}}$ and $\lambda_{\mathrm{ub}}$ are set by the user, with the only condition that the main lobe should not be included in their interval. The purpose of this window is to first, compensate for the decaying factor of the side-lobes and create closer to delta responses in the Fourier domain (the $(\alpha - \alpha_B)^2$ term), and second, to lower the spectral leakage of the local peaks in the Fourier domain (the Hann window). Applying this window and taking the Fourier transform of Eq. (9) (neglecting the last term) leads to:

$$\mathscr{F}\{R_c\} \approx \mathscr{F}\{R_s\} + \mathscr{F}\{\psi_o w\} + \mathscr{F}\{\psi_1 w\}e^{\pm j\theta_1}\delta(\omega \mp (2M - 2t + 2)) - \mathscr{F}\{\psi_2 w\}e^{\pm j\theta_2}\delta(\omega \mp (2t-2)) \tag{11}$$
$$+ \mathscr{F}\{\psi_3 w\}e^{\pm j\theta_3}\delta(\omega \mp (2M - 2t)) - \mathscr{F}\{\psi_4 w\}e^{\pm j\theta_4}\delta(\omega \mp (2t)) + \mathscr{F}\{\psi_5 w\}e^{\pm j\theta_5}\delta(\omega \mp (2)).$$

As it can be seen from Eq. (11), the new frequencies project themselves as new peaks in the amplitude of the Fourier transform of the reflection spectrum. Therefore, regardless of the amplitude of the individual $\mathscr{F}\{\psi_i w\}$ terms, for a perfectly produced sensor (with little bi-refringence), the mere existence of such high amplitude peaks in the range of

$\omega = 0$ to $\omega = 2M$ indicates sudden changes in the strain field, and possibly crack formation along the length of the sensor. It is noteworthy that the local peaks which are not spatially separated enough (meaning $\omega = 2t$ and $\omega = 2t-2$, $\omega = 2M-2t+2$ and $\omega = 2M-2t$, and $\omega = 2$ and $\omega = 0$) are usually overlapped and form a single local peak due to spectral smearing. Also note the ever-present high amplitude peak at $\omega = 1000$ in $\mathscr{F}\{R_s\}$ in Eq. (11).

A simulated example of this phenomenon is shown in Fig. 2 where a sensor of length 10 mm with a nominal Bragg wavelength of 1550 nm was designed to be in contact with a crack at position 2.5 mm from its start (the same structure as Fig. 1, except having only the first crack at $z = 2.5$ mm position). The structure was assumed to have $M = 500$ segments, therefore the crack tip was located at $t = 125$. From Eq. (11) it is expected, from the amplitude graph, to have peaks at locations $\omega = \{0, 250, 750, 1000\}$, which is evident in Fig. 2c. For comparison, the amplitude of the Fourier transform of the side-lobes of an unstressed sensor is depicted as well, with its peaks at $\omega = \{0, 1000\}$.

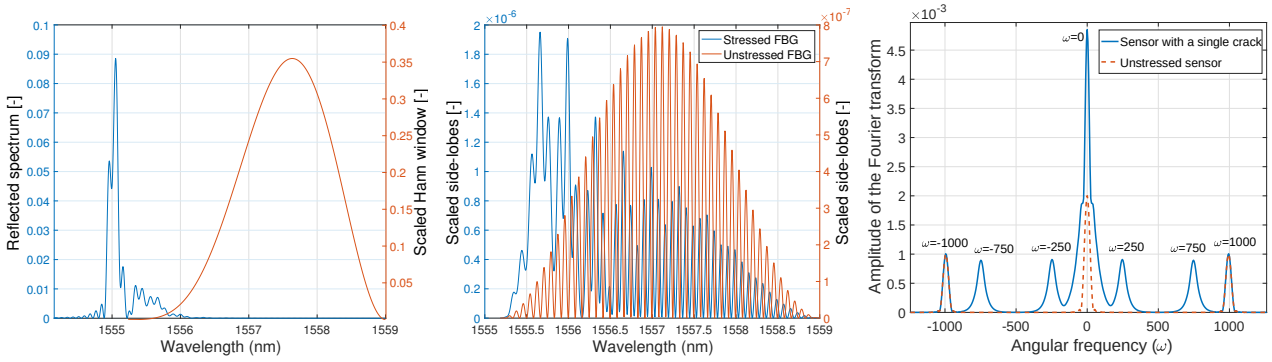


(a) (b) (c)

Fig. 2. (a): Reflection spectra of a sensor near a crack and the scaled Hann window. (b): Windowed side-lobes of the reflection spectra. (c): Fourier transform of the windowed side-lobes for both stressed and unstressed sensors.

Note that the effect of formation of cracks at other segments (or an increase in the crack density) is an increased number of terms in the summation term of Eq. (8), and therefore, more local peaks in the amplitude spectrum of Eq. (11). By inspection of Fig. 2c, it can be seen that there is a clear difference between the Fourier transform of the side-lobes of a sensor in proximity of cracks, and that of a sensor under smoothly varying strain fields. This difference can be utilised to design a simple threshold level based classifier in order to detect cracks.

## 4. Conclusions

In this paper, using the properties of the newly developed ATMM model, we showed the potential of using the information in the side-lobes of the reflection spectra of FBG sensors to detect cracks along the length of embedded FBGs between the layers of composite structure. Simulation results showed a clear correspondence between the angular frequency of the local peaks in the Fourier transform of the side-lobes of an FBG with a single crack, and those extracted from the mathematical model.

## References

1. A. D. Kersey, M. A. Davis, H. J. Patrick, M. LeBlanc, K. P. Koo, C. G. Askins, M. A. Putnam, and E. J. Friebele, "Fiber grating sensors," Journal of Lightwave Technology, **15**, 1442-1463 (1997).
2. T. H. Loutas, A. Panopoulou, D. Roulias, and V. Kostopoulos, "Intelligent health monitoring of aerospace composite structures based on dynamic strain measurements," Expert Syst Appl., **39(9)**, 8412-8422 (2012).
3. A. Rajabzadeh, R. C. Hendriks, R. Heusdens, and R. M. Groves, "Classification of composite damage from FBG load monitoring signals," Proceedings of SPIE, 10168, 1016831 (2017).
4. L. N. McCartney,"Theory of stress transfer in a 0-90-0 cross-ply laminate containing a parallel array of transverse cracks," Journal of the Mechanics and Physics of Solids, **40**, 27-68 (1997).
5. A. Rajabzadeh, R. Heusdens, R. C. Hendriks, and R. M. Groves,"Calculation of the mean strain of non-uniform strain fields using conventional FBG sensors," arXiv:1803.08139 (2018).
6. A. Yariv, "Coupled-mode theory for guided-wave optics," Quantum Electronics, **9(9)**, 919–933 (1973).
7. M. Yamada, and K. Sakuda, "Analysis of almost-periodic distributed feedback slab waveguides via a fundamental matrix approach," Applied Optics, **26(16)**, 3474-3478 (1987).